Nuclear Instruments and Methods in Physics Research A 1056 (2023) 168626

Contents lists available at ScienceDirect

Nuclear Inst. and Methods in Physics Research, A

journal homepage: www.elsevier.com/locate/nima

Full Length Article

Characterization of large diameter dual-mode cerium-doped Tl_2LiYCl_6 advanced scintillator

R. Hawrami [a,*], E. Ariesanti [a], A. Burger [a], E. Neely [a], J. Glodo [b], L. Pandian [b], C. Ji [b], S. Stepanoff [c], D.E. Wolfe [c], F. Liang [d]

[a] Fisk University, Nashville, TN 37208, United States of America
[b] Radiation Monitoring Device, Inc., Watertown, MA 02472, United States of America
[c] Penn State University, State College, PA 16802, United States of America
[d] Teledyne FLIR, Oak Ridge, TN, United States of America

ARTICLE INFO

Keywords:
Bulk crystal growth
Gamma-ray detector
Neutron detector
Dual mode scintillation detector
Thallium-based elpasolite crystals

ABSTRACT

In this paper we are reporting on the progress and scale up of the Cerium-doped Tl_2LiYCl_6 (TLYC) scintillator. The boules up to 2-inch in diameter were grown by the Bridgman method at Fisk University. The lapped and polished samples were characterized for their scintillation properties including gamma-neutron dual mode detection. The 1.5-inch diameter samples demonstrated the energy resolution as good as 4.5% (FWHM) at 662 keV. The neutron peak due to ^{6}Li(n, α) reaction was observed at 1.8 MeV gamma equivalent energy. Gamma-neutron pulse shape discrimination (PSD) was demonstrated with the Figure-of-Merit (FOM) of 1.8. The hermetically encapsulated samples were also evaluated for their radiation hardness with irradiation up to 1 Mrad.

1. Introduction

Interest in elpasolite scintillator crystals has recently increased due to their versatility and favorable optical and scintillation properties as dual mode gamma-neutron detection materials. Compositions that contain lithium (Li) have been especially investigated intensively for their ability to detect both thermal neutrons and gamma photons in a single inorganic crystal [1–4]. In these crystals scintillation is typically triggered by using an activator, such as cerium (Ce) or Ce co-doped with other lanthanides or alkalides. While excellent, Cs-based elpasolites suffer from lower density and detection efficiency comparable to that of NaI. Therefore, recently several materials, including elpasolites, have been investigated where Cs ions have been substituted with Tl ion to achieve higher detection efficiency. For example, substitution of Cs with Tl in Cs_2 $LiYCl_6$ (CLYC) led to creation of Tl_2 $LiYCl_6$ (TLYC). This substitution increased the material's effective atomic number Z_{eff} from 45 to 69 and the density from 3.3 to 4.5 g/cm^3 [5–8]. The intrinsic detection efficiency for a $\varnothing 1'' \times 1''$ crystal irradiated with 662 keV gamma-rays also increases from 46.5% for CLYC to 65.4% for TLYC. TLYC, as a Tl-based elpasolite, is usually doped with cerium to improve luminescent and decay time [5]. However, Tl^+ is also a luminescent ion and thus, a competition between the two centers (Tl^+ and Ce^{3+}) can occur [5,9]. Besides having a better detection efficiency, TLYC has a lower melting point, higher photo fraction, higher light yield, shorter decay time constants compared to CLYC [6]. TLYC has been invested over last few years as a potential dual mode scintillator [5–11], however, larger crystals necessary for the instrumentation, have not been fully developed.

For the past two years Fisk University has been focused on improving the material and growth properties of TLYC. While favorable properties of TLYC are very attractive, issues surrounding its growth process, especially in larger (≥1-inch) diameters, have still been a concern. Growing elpasolite crystals in general usually requires binary compounds as starting materials, including dopants. Reactions between these binaries create undesirable additional phases in the melt and, eventually, crystal. Hence incongruency in melt grown elpasolite crystals is an issue. When the growth is incongruent, the growth yield is low, which increases the overall production cost. Elimination of these additional phases can be accomplished if the crystal grower knows the behavior of these phases well, usually with the aid of phase diagrams.

* Corresponding author.
E-mail addresses: rhawrami@fisk.edu (R. Hawrami), eariesanti@fisk.edu (E. Ariesanti), aburger@fisk.edu (A. Burger), eneely1@myfiskedu.onmicrosoft.com (E. Neely), jglodo@rmdinc.com (J. Glodo), lspandian@rmdinc.com (L. Pandian), cji@rmdinc.com (C. Ji), sps5764@arl.psu.edu (S. Stepanoff), dew125@arl.psu.edu (D.E. Wolfe), Felix.Liang@teledyneflir.com (F. Liang).

https://doi.org/10.1016/j.nima.2023.168626
Received 8 June 2023; Received in revised form 5 August 2023; Accepted 15 August 2023
Available online 18 August 2023

Elpasolite scintillators also depend on dopants to create the necessary energy levels to promote or improve scintillation. Ce is one of the most common dopants. Non-uniformity in dopant distribution causes dissimilar scintillation performance from different parts of the crystal boule, which decreases usable crystal volume. All these detrimental factors not only decrease growth yield, but they also influence the overall cost to produce elpasolite scintillators. Most of elpasolite crystals like TLYC are also hygroscopic, thus requiring proper handling procedures and hermetic packaging to preserve the crystals.

This paper reports on the most recent progress in large diameter growth of Ce-doped TLYC crystals, and results of their characterization as a dual-mode gamma-neutron scintillator. We also report on an initial study of their radiation hardness.

2. Experimental methods

2.1. Growth

The Bridgman growth method [5–8] was employed to grow large diameter TLYC crystals at Fisk University. The same growth procedure was followed for all growth ampoule sizes. The growth process was started by purchasing high purity (>99.999%) starting compounds from chemical vendors. Stoichiometric amounts of TlCl, LiCl, YCl_3, and $CeCl_3$ were placed inside a pre-cleaned fused silica growth ampoule that was subsequently connected to a high vacuum pump. After the required vacuum level was reached ($<10^{-3}$ Torr), the ampoule was sealed and then placed in a two-zone vertical ampoule for growth. The growth speed was 5–10 mm/h and the cooling down speed was 20 °C/h. All TLYC material evaluated in this paper was produced at Fisk University.

2.2. Post-growth processing and encapsulation work

After growth each TLYC boule was retrieved and underwent post-growth processing, which includes cutting, lapping, and polishing. Lapping and polishing were accomplished with Al_2O_3 or SiC polishing pads up to 1200 grit. Due to the crystal being hygroscopic, the processing was done in mineral oil when done in non-dry/inert atmosphere or dry when done inside an inert (argon) atmosphere glove box. To avoid crystal degradation, encapsulation of TLYC crystals were done inside the glove box. Moisture was removed from encapsulation parts surfaces by placing them in vacuum inside the antechamber of the glove box for a period up to twenty-four hours. Custom aluminum containers were fabricated in house at Fisk University to accommodate different sizes and shapes of crystals. Two types of optical windows, quartz (index of refraction $n_d = 1.46$) and sapphire ($n_d = 1.77$), were utilized. After the final polish, each crystal was wrapped using Teflon tape and Gore® Teflon pad as reflectors. One face of the crystal was open for mounting to the optical window using silicone optical grease as coupling. The aluminum container was then hermetically sealed.

2.3. Characterization

For initial characterization at Fisk University, a TLYC sample was immersed in mineral oil placed in a straight-sided quartz cup lined with Teflon tape and covered with a Gore® pad [5–8]. The cup was coupled to a photomultiplier tube with a thin layer of optical grease. A R6231-100 Hamamatsu super bi-alkali photomultiplier tube (PMT), connected a 2005 Canberra preamplifier and a 2022 Canberra amplifier, was utilized. For gamma-ray spectra collection, the PMT was operated at −700 V bias. Pulse height spectra from gamma-ray check sources such as ^{137}Cs, ^{152}Eu, and ^{241}Am were collected, from which energy resolution, relative light yield data, and non-proportionality data were derived. To obtain luminescence decay time information, each sample was irradiated with a ^{137}Cs check source. With the PMT biased at −1200 V, the signals from the anode were recorded with a CAEN DT5720C digitizer and the waveforms were analyzed offline.

Samples of TLYC crystals grown and processed at Fisk were sent to three collaborators to corroborate measurements, for further characterization with thermalized neutron sources, and for a radiation hardness study. A ∅1.5″ × 1.5″ TLYC crystal (grown and cut at Fisk) were sent to Radiation Monitoring Devices, Inc. (RMD) for testing with a thermalized Am-Be neutron source. Prior to characterization the crystal was lapped, polished, and hermetically encapsulated. The encapsulated crystal was coupled to a Hamamatsu R6233-100 super-bialkali PMT and associated NIM equipment. Gamma-ray characterization using a ^{137}Cs check source and collection of energy-equivalent Am-Be spectra were done for several amplifier shaping times. With the PMT biased at −1200 V, the anode signals were collected with a CAEN 5720 digitizer. The waveforms were analyzed off-line to determine the pulse shape discrimination (PSD) of the gamma and neutron events and calculate Figure-of-Merit (FOM) [12], which quantitatively measures the separation between gamma and neutron events.

Another hermetically encapsulated ∅1″ × 1″ TLYC sample (from an early large diameter TLYC crystal boule prior to growth optimization) was sent to Teledyne FLIR (FLIR) for characterization with a thermalized ^{252}Cf neutron source. The encapsulated crystal was coupled to a Hamamatsu R6231-100 super-bialkali PMT and associated NIM equipment. The waveforms from the PMT anode were analyzed to determine PSD of the gamma and neutron events and calculate FOM.

Lastly, a hermetically encapsulated 17 × 17 × 25 mm^3 TLYC sample was sent to Penn State University (PSU) for an initial radiation hardness study. This study was intended to determine whether this novel material could be employed in high-dose radiation fields. The encapsulated crystal was irradiated with a ^{60}Co gamma source at a dose rate of 155 krad/h at intervals of 0.001, 0.01, 0.1, 0.5, and 1.0 Mrad air dose (i.e.,10 Sv, 100 Sv, 1 kSv, 5 kSv, and 10 kSv air dose). Between each irradiation step, a photographic image of the crystal was taken. Post-irradiation the crystal was coupled to Hamamatsu H10580 PMT assembly that was connected to Canberra 2007 preamplifier and Canberra 2022 shaping amplifier. Due to logistical constraints at the time, only spectra after irradiation at 0.1 Mrad were collected. ^{137}Cs spectra were collected with the PMT operated at −650 V with 2 μs amplifier shaping time.

3. Results and analysis

3.1. Growth, encapsulation, and gamma-ray characterization results at Fisk

Fig. 1 shows the latest ∅1.5-inch and ∅2-inch TLYC crystal boules grown at Fisk, showing single, crack-free, and transparent boules. Fig. 2 (a) shows a ^{137}Cs spectrum collected with a ∅1.5″ × 1.5″ TLYC crystal encapsulated in a temporarily sealed can (inset picture). The energy

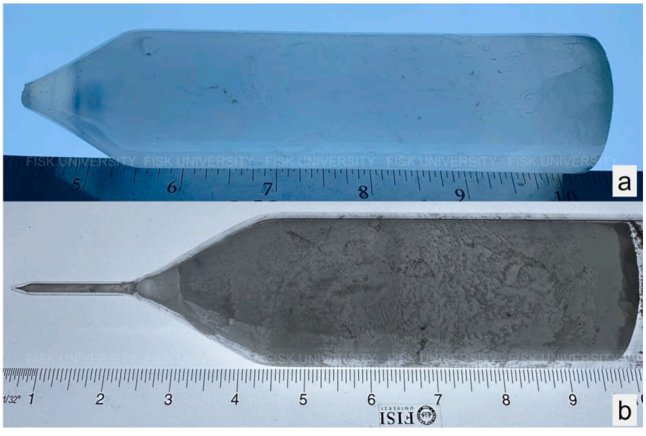

Fig. 1. Examples of the latest (a) ∅1.5-inch and (b) ∅2-inch TLYC single crystal boules grown at Fisk.

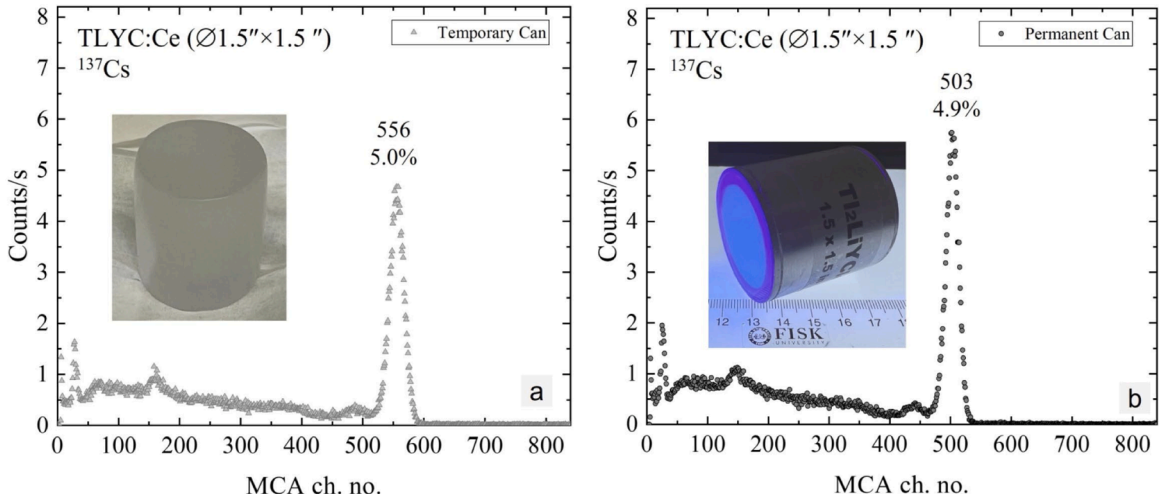

Fig. 2. (a) ^{137}Cs spectrum collected with a ∅1.5″ × 1.5″ TLYC sample encapsulated in a temporary can. (b) ^{137}Cs spectrum collected with the same ∅1.5″× 1.5″ TLYC sample but encapsulated in a permanently sealed hermetic can.

resolution of 5.0% (FWHM) was measured for the 662 keV full energy peak. The crystal was then hermetically encapsulated in a permanently sealed can (inset picture in Fig. 2(b)). ^{137}Cs spectrum was collected with the crystal in the hermetic encapsulation, with a measured energy resolution of 4.9% (FWHM). While the relative light yield of the crystal in the permanent can (662 keV peak position at channel number 503 in Fig. 2(b)) was about 9.5% lower compared to when it was temporarily sealed (662 keV peak position at channel number 556 in Fig. 2(a)), the energy resolution of was slightly better. In both cases the peak is associated with a satellite peak at lower energy due to Tl K_α escape X-ray (escape peak, ∼73 keV). Note that due to the larger size of the crystal, more full energy absorption events occur instead of escape events.

3.2. Evaluation of TLYC:Ce at RMD

RMD received from the Fisk University a ∅1.5 in diameter and over 2-inch long boule of TLYC. Fig. 3 shows the sample after lapping and polishing at RMD. This boule was used to produce multiple samples, including 13 × 10 × 10 mm^3 cuboid and a ∅1.5″ × 1″ cylinder. The results from evaluation of these samples are provided below.

Fig. 4 shows the characterization results of a 13 × 10 × 10 mm^3 TLYC sample that was encapsulated in a temporarily sealed can and tested as a dual mode detector. ^{137}Cs spectra collected with different amplifier shaping times were collected. Fig. 4(a) shows ^{137}Cs spectrum collected with 2 μs amplifier shaping time with the best energy resolution of 4.4% (FWHM) for the full energy peak at 662 keV. Fig. 4(b) shows Am-Be spectra with the best energy resolution for the peak due to thermal neutron events measured at 3.2% (FWHM) for the gamma equivalent energy (GEE) of 1.77 MeV. Fig. 4(c) shows the PSD plot created using the waveforms generated by thermalized Am-Be neutron source. This plot shows clear separation of the neutron counts (x = 125; y = 0.36) from the gamma continuum at the bottom of the graph. Projection of the events in x = (106, 300) range of the scatter plot results in FOM of 1.9 (Fig. 4(d)). The separation is sufficiently high for an effective gamma-neutron discrimination.

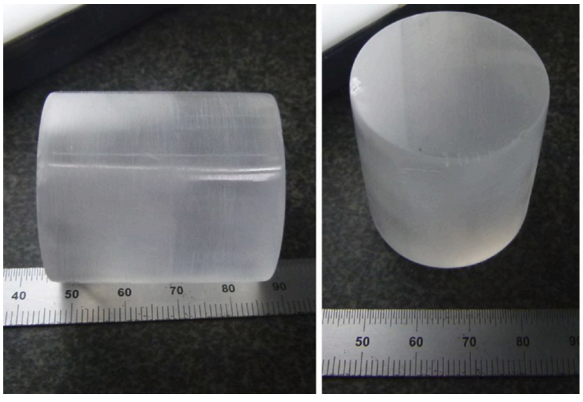

Fig. 3. A ∅1.5″ × 2″ TLYC sample, lapped and polished at RMD, from a boule grown at Fisk.

Fig. 5 shows the characterization results of a larger ∅1.5″ × 1″ TLYC sample that was encapsulated in a permanently sealed can. Fig. 5(c) shows a photograph of the encapsulated TLYC sample. Fig. 5(a) shows a ^{137}Cs spectrum collected with 1 μs amplifier shaping time, with the best energy resolution of 4.4% (FWHM) for the full energy peak at 662 keV. Fig. 5(b) shows Am-Be spectra collected with the best energy resolution for the peak due to thermal neutron events measured at 5.2% (FWHM) for the gamma equivalent energy (GEE) of 1.76 MeV. Fig. 5(d) shows the PSD scatter plot created using the waveforms generated by thermalized Am-Be neutron source in the TLYC crystal. Projection of the events in x = (116, 371) region in the scatter plot results in FOM of 1.8 (Fig. 5(e)).

Since these two samples have significantly different volumes (1.3 cm^3 vs. 29 cm^3) it is interesting to make some comparisons. The best energy resolution at 662 keV is the same. However, the resolution degrades somewhat with longer shaping time for the larger sample. This would suggest some level of non-uniformity still present in the boule. This is further confirmed by the resolution and shape of the thermal neutron peak, which is less symmetric in the larger sample. The PSD scatter plot also indicates some variation in the material. Since we expect the energy resolution to improve with a longer shaping time, good energy resolution at 1 or 2 μs suggests the material can be further improved and potentially reach sub 4% level. It is also worth noting the intensity of the escape peak: while the small sample shows a well-separate clear escape peak, in the larger sample this peak is barely visible. The peak-to-Compton value is 3.5 for the small sample, and 4.8 for the larger one. The peak-to-Compton value for the full 1.5″ right cylinder (Fig. 2(b)) is above 11.

3.3. Measurements for one inch Ce-doped TLYC (FLIR)

Fig. 6 shows the PSD analysis conducted at FLIR on a ∅1″ × 1″ TLYC crystal (from an early large diameter TLYC crystal boule prior to growth optimization) that was grown, processed, and permanently

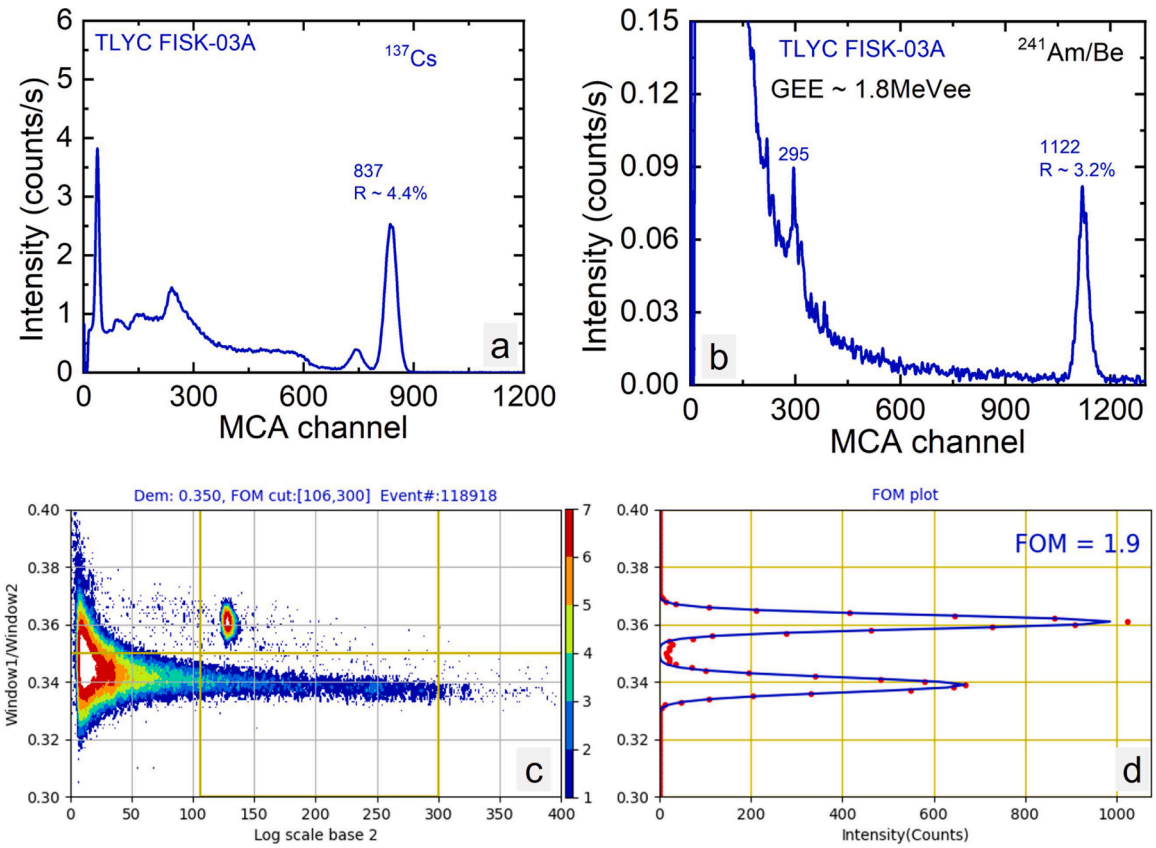

Fig. 4. Characterization of a $13 \times 10 \times 10$ mm^3 TLYC crystal (grown and pre-processed at Fisk), encapsulated in a temporary can as a dual mode detector, conducted at RMD (a) ^{137}Cs spectra collected with 2 μs amplifier shaping times. (b) Energy equivalent Am-Be spectra collected with 2 μs amplifier shaping times. (c) PSD scatter plot created using the waveforms generated by thermalized Am-Be neutron source in the TLYC crystal. (d) Projection of the events in [106, 300] region in the scatter plot results in FOM of 1.9.

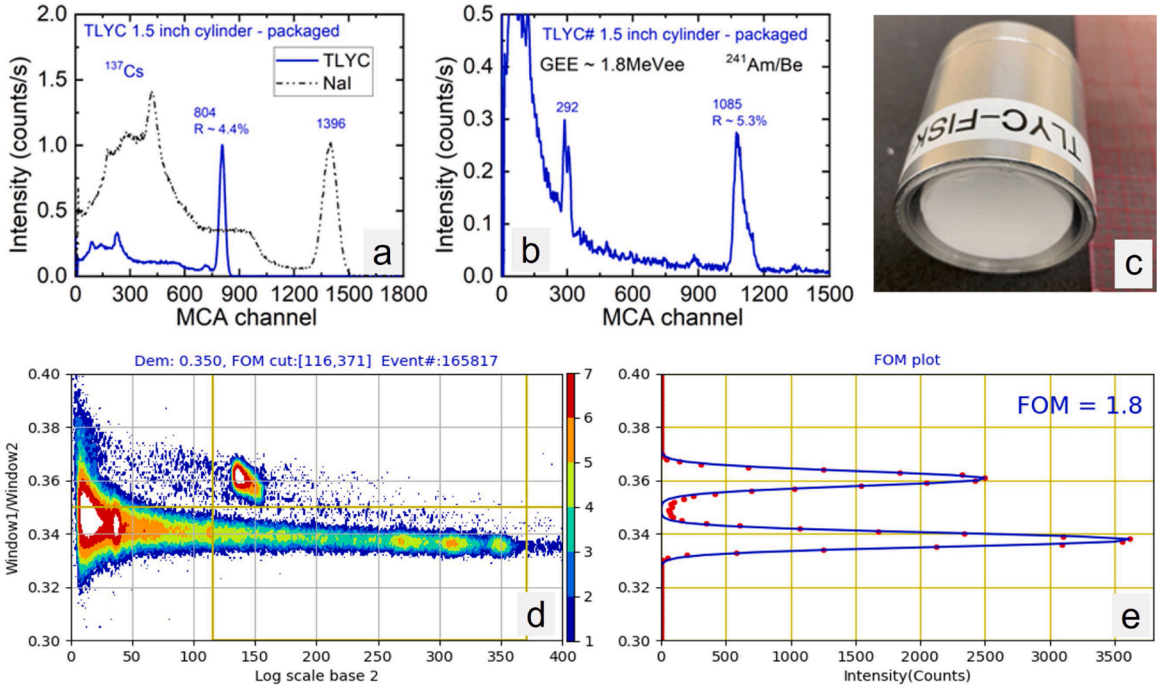

Fig. 5. Characterization of a $\varnothing 1.5'' \times 1''$ TLYC sample, encapsulated in a permanently sealed can as a dual mode detector. (a) ^{137}Cs spectra collected with 1 μs amplifier shaping time. (b) Energy equivalent Am-Be spectra collected with 1 μs amplifier shaping time. (c) Polished crystal. (d) PSD scatter plot created using the waveforms generated by thermalized Am-Be neutron source in the TLYC crystal. (e) Projection of the events in [116, 371] region in the scatter plot results in FOM of 1.8.

encapsulated at Fisk. Fig. 6(a) shows the PSD scatter plot created using the waveforms generated in the TLYC crystal from the irradiation with a thermalized ^{252}Cf neutron source. Projection of the events within the box in the scatter plot results in FOM of 1.4 (Fig. 6(b)). Compared to the FOM in Fig. 6(b), Figs. 4 and 5 show that improvements in the crystal quality improve crystal performance.

3.4. Initial radiation hardness measurements at Penn State

Irradiation of the hermetically sealed 17 × 17 × 25 mm^3 TLYC:Ce crystal was carried out at the Radiation Science and Engineering Center (RSEC) at Penn State University using ^{60}Co gamma radiation sources that surround the samples in a lead-shielded chamber. At the time of the experiment, the ^{60}Co sources provided an isotropic dose at a constant rate of 155 krad/h or 1.55 kSv/h (air) in an ambient environment. The sample were placed within a ∅4″ × 4″ cylindrical region inside the center of the irradiation chamber, where the overall uncertainty of the dose rate is +/−2.4% at a 95% confidence level, which is certified using the Fricke dosimetry system by the National Voluntary Laboratory Accreditation Program (NVLAP) under the National Institute of Standards and Technology (NIST).

Fig. 7 shows how the TLYC:Ce crystal darkens as a function of absorbed gamma dose possibly due to the production of F-centers, which are anionic vacancies that readily form in alkali halides upon interaction with ionizing radiation. The production of F-centers is associated with the absorption of visible wavelengths of light due to the quantization of electrons trapped in the halide vacancies, which may manifest as a darker appearance of the TLYC:Ce crystal. These absorbing and scattering centers in the crystal will readily cause light loss and increase decay time, reducing the efficiency of the scintillation mechanism and causing afterglow phenomena, which is apparent in Fig. 7, where scintillation is perceptible for several minutes after removal from the gamma source.

Fig. 8 shows the characterization of the 17 × 17 × 25 mm^3 hermetically encapsulated TLYC crystal at Fisk University before and after the irradiation at Penn State University. Fig. 8(a) shows ^{137}Cs spectra collected by the encapsulated TLYC crystal before and after irradiation as well as after repackaging (all measurements were done at Fisk University). Prior to shipment to Penn State University (before irradiation) energy resolution of 5.9% (FWHM) was measured for the full energy peak at channel number 479. After the crystal was shipped back to Fisk University (as-received and after irradiation), energy resolution of 15.6% (FWHM) was measured for the 662 keV peak. The full energy peak was now measured at channel number 71 (i.e., 15% of the original light yield). After repolishing and repackaging, energy resolution of 14.5% was measured for the full energy peak, now measured at channel number 161 (34% of the original light yield). The temporal data is shown in Fig. 8(b). Decay time constants calculated from the temporal data prior to irradiation were 0.05 μs (5%), 0.46 μs (60%), and 1.73 μs (35%), while the decay constants after irradiation and repackaging were calculated to be 0.04 μs (10%), 0.47 μs (54%), and 2.36 μs (36%).

As seen in Fig. 7, there was a progression in the yellowing of the encapsulation crystal with the increase in irradiation dose. This yellowing may be due to the reaction of the crystal with the organic epoxy used to encapsulate the crystal. The irradiation may have also disintegrated the organic epoxy, rendering it ineffective to seal the crystal from moisture. Further analysis study will be performed on more encapsulated samples free of organic chemicals. More radiation hardness study, with better preparation and on-site analysis, will be needed to completely understand the reduction in crystal performance after a high dose of gamma radiation.

4. Conclusions

We reported on the progress and scale up of advanced Cerium-doped Tl_2LiYCl_6 (TLYC) scintillator up to 2-inch in diameter crystals grown by the Bridgman method at Fisk University. The lapped and polished samples of 1-inch and 1.5-inch diameter TLYC crystals were successfully encapsulated and characterized for their scintillation properties including gamma-neutron dual mode detection. The 1.5-inch diameter samples demonstrated the energy resolution as good as 4.5% (FWHM) at 662 keV. The neutron peak due to ^{6}Li(n, α) reaction was observed at 1.8 MeV gamma equivalent energy. Gamma-neutron pulse shape discrimination (PSD) was demonstrated with the Figure-of-Merit (FOM) of 1.8. The hermetically encapsulated samples were also evaluated for their radiation hardness with irradiation up to 1 Mrad. While the post irradiated crystal show signs of deterioration, it is not clear whether this effect was caused by direct irradiation damage or caused by the failure of the encapsulation during irradiation, which may have exposed the moisture sensitive crystal to air. Careful rumination on the packaging procedure and/or choices of packaging materials will be studied and reported in the future.

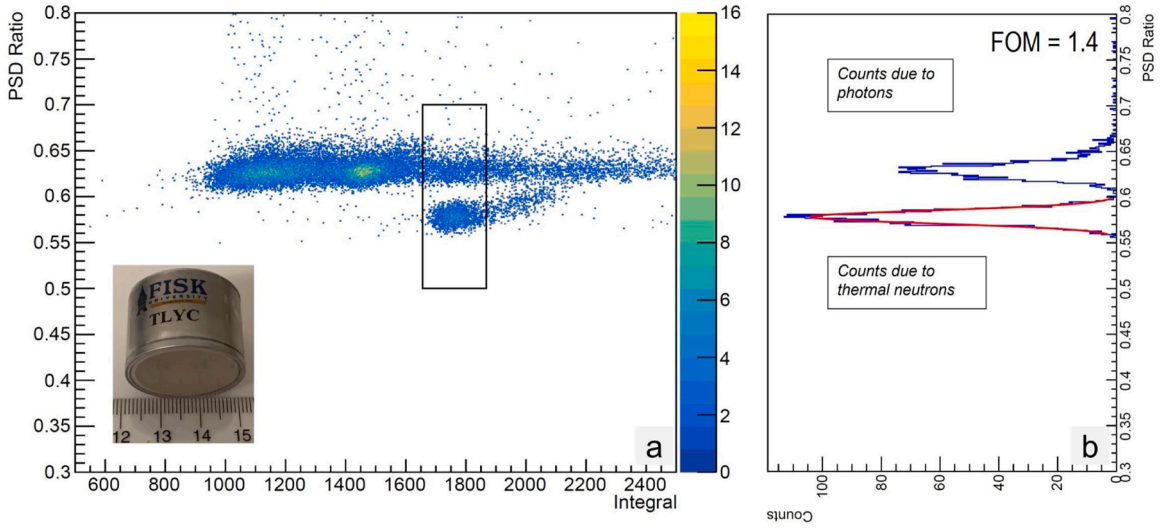

Fig. 6. Characterization of on a ∅1″ × 1″ TLYC crystal (grown, processed, and hermetically encapsulated at Fisk) conducted at FLIR (a) PSD scatter plot created using the waveforms generated by thermalized ^{252}Cf neutron source in the TLYC crystal. (b) Projection of the events enclosed in the box shown in the scatter plot results in FOM of 1.4.

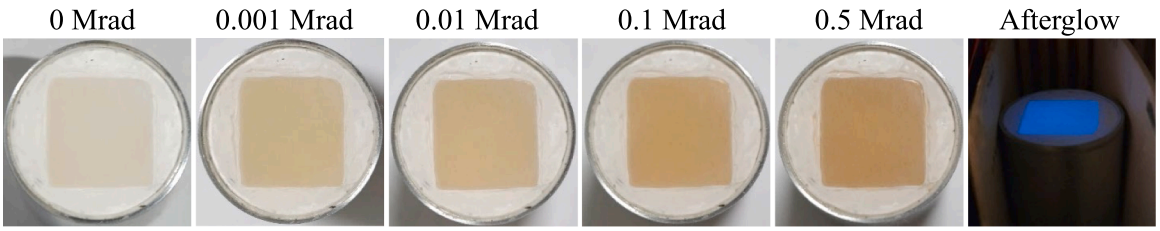

Fig. 7. Digital images of TLYC as a function of absorbed gamma dose from ^{60}Co sources using an air reference. After each exposure, the crystal continued to luminesce after removal from the radiation environment.

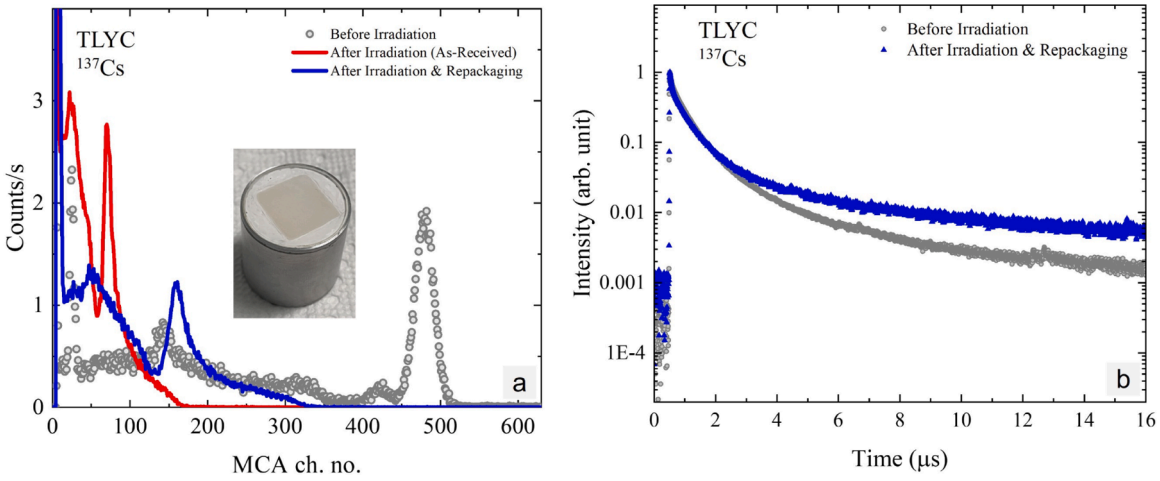

Fig. 8. Before and after radiation hardness test measurements at Fisk on the 17 × 17 × 25 mm^3 hermetically encapsulated TLYC crystal (a) ^{137}Cs spectra collected by the encapsulated TLYC crystal: before irradiation, as received after irradiation, and after repackaging. Inset picture: the encapsulated TLYC crystal prior to shipment to Penn State. (b) Temporal data collected by the TLYC crystal before irradiation and after irradiation & repackaging.

Declaration of competing interest

The authors declare that they have no known competing financial interests or personal relationships that could have appeared to influence the work reported in this paper.

Data availability

Data will be made available on request.

Acknowledgments

This work is supported in part by Defense Threat Reduction Agency Interaction of Ionizing Radiation with Matter University Research Alliance, United States of America (DTRA IIRM URA) Cooperative Agreement # HDTRA1-20-2-0002. E. Neely is currently a graduate student at the University of Michigan, Ann Arbor, MI (eneely@umich.edu). F. Liang is currently with Los Alamos National Laboratory, Los Alamos, NM 87545 (jfliang@lanl.gov).

References

[1] J. Glodo, R. Hawrami, K.S. Shah, Development of Cs_2LiYCl_6 scintillator, J. Cryst. Growth 379 (2013) 73–78, https://doi.org/10.1016/j.jcrysgro.2013.03.023.
[2] M.B. Smith, et al., Fast neutron measurements using Cs_2LiYCl_6: Ce (CLYC) scintillator, Nucl. Instrum. Methods Phys. Res. Sec. A 784 (2015) 162–167, https://doi.org/10.1016/j.nima.2014.09.021.
[3] J. Glodo, et al., New developments in scintillators for security applications, Physics Procedia 90 (2017) 285–290, https://doi.org/10.1016/j.phpro.2017.09.012.
[4] U. Shirwadkar, R. Hawrami, J. Glodo, E. van Loef, K.S. Shah, Novel scintillation material $Cs_2LiLaBr_{6-x}Cl_x$:Ce for gamma-ray and neutron spectroscopy, in: Presented at the IEEE Nuclear Science Symposium Conference Record, 2012, pp. 1963–1967, https://doi.org/10.1109/NSSMIC.2012.6551453.
[5] E. Ariesanti, et al., Effects of cerium concentration in Tl_2LiYCl_6 scintillation detectors, in: 2016 IEEE Nuclear Science Symposium, Medical Imaging Conference and Room-Temperature Semiconductor Detector Workshop, NSS/MIC/RTSD, Strasbourg, France, 2016, pp. 1–2, https://doi.org/10.1109/NSSMIC.2016.8069843.
[6] R. Hawrami, E. Ariesanti, L. Soundara-Pandian, J. Glodo, K.S. Shah, Tl_2LiYCl_6: Ce: A new elpasolite scintillator, IEEE Trans. Nucl. Sci. 63 (6) (2016) 2838–2841, https://doi.org/10.1109/TNS.2016.2627523.
[7] R. Hawrami, E. Ariesanti, H. Wei, J. Finkelstein, J. Glodo, K. Shah, Tl_2LiYCl_6: Large diameter, high performing dual mode scintillator, Crystal Growth Des. 17 (7) (2017) 3960–3964, https://doi.org/10.1021/acs.cgd.7b00583.
[8] R. Hawrami, E. Ariesanti, A. Burger, P. Sellin, Latest growth of large diameter Tl-based elpasolite scintillation crystals, Opt. Mater. 128 (2022), 112324, https://doi.org/10.1016/j.optmat.2022.112324.
[9] F. Moretti, D. Onken, D. Perrodin, E. Bourret, Investigation of the competition between Tl^+ and Ce^{3+} scintillation in Tl_2LiYCl_6: Ce, an elpasolite scintillator, J. Lumin. 241 (2022), 118549, https://doi.org/10.1016/j.jlumin.2021.118549.
[10] D.R. Onken, D. Perrodin, E.D. Bourret, C. Vogel, The crystal structure and temperature dependence of the elpasolite Tl_2LiYCl_6, p. 26.
[11] M.M. Watts, K.E. Mesick, K.D. Bartlett, D.D.S. Coupland, Thermal characterization of Tl_2LiYCl_6: Ce (TLYC), IEEE Trans. Nucl. Sci. 67 (3) (2020) 525–533, https://doi.org/10.1109/TNS.2020.2972529.
[12] R.A. Winyard, J.E. Lutkin, G.W. McBeth, Pulse shape discrimination in inorganic and organic scintillators. I, Nucl. Instrum. Methods 95 (1) (1971) 141–153, https://doi.org/10.1016/0029-554X(71)90054-1.